

Continuous-space automaton model for pedestrian dynamicsGabriel Baglietto^{1,2} and Daniel R. Parisi^{3,4,*}¹*Facultad de Ingeniería, UNLP, Calle 1 esquina 47, 1900 La Plata, Argentina*²*Instituto de Física de Líquidos y Sistemas Biológicos (IFLYSIB), Calle 59 Nro. 789, 1900 La Plata, Argentina*³*Instituto Tecnológico de Buenos Aires, 25 de Mayo 444, 1002 C. A. de Buenos Aires, Argentina*⁴*Consejo Nacional de Investigaciones Científicas y Técnicas, Rivadavia 1917, 1033 C. A. de Buenos Aires, Argentina*

(Received 24 December 2010; published 23 May 2011)

An off-lattice automaton for modeling pedestrian dynamics is presented. Pedestrians are represented by disks with variable radius that evolve following predefined rules. The key feature of our approach is that although positions and velocities are continuous, forces do not need to be calculated. This has the advantage that it allows using a larger time step than in force-based models. The room evacuation problem and circular racetrack simulations quantitatively reproduce the available experimental data, both for the specific flow rate and for the fundamental diagram of pedestrian traffic with an outstanding performance. In this last case, the variation of two free parameters (r_{\min} and r_{\max}) of the model accounts for the great variety of experimental fundamental diagrams reported in the literature. Moreover, this variety can be interpreted in terms of these model parameters.

DOI: [10.1103/PhysRevE.83.056117](https://doi.org/10.1103/PhysRevE.83.056117)

PACS number(s): 89.40.-a, 45.70.Vn, 89.65.-s

I. INTRODUCTION

The movement of people and crowds is an important field of research that has gained interest due to the increasing need to design safer and more comfortable pedestrian facilities. Traditionally, crowd movements were studied by engineers with sizing purposes when designing buildings and transport systems for people [1–3]. Since the 1990s this subject has been studied with the aid of computer simulations, and several models have been presented. A general classification of pedestrian models can be found in [4], and they can be classified into rule based and force based, discrete and continuous, etc.

In rule-based models the state of the system evolves following predefined rules, which are applied on individual agents. Usually, this kind of model considers a discretization of space into a grid, as is the case of cellular automata (CA) models. Some emblematic CA models are the floor field [5] and lattice gas [6] models. On the other hand, in force-based models pedestrians are considered as particles that interact by means of forces, and so the state of the system is governed by Newton's equation. In general, the space and state of the particles are considered continuous in this kind of model. Examples of force-based models are the social force model [7,8] and the centrifugal force model [9,10].

Each approach has benefits and shortcomings. For example, discrete-space CA model simulations are faster, but they present inconsistencies when computing distance (and thus velocities), as clearly stated in [11]. On the contrary, force-based model simulations are more expensive but allow describing trajectories and velocities correctly. Besides, realistic forces and pressure can be estimated.

We present here a model summarizing the best of the two previously described approaches: the contractile particle model (CPM). The CPM is a continuous-space automaton inspired by models of self-propelled pointlike particles like those described in [12–14]. Antecedents of this hybrid ap-

proach are, for example, the mobile lattice gas model [11] and the work of Thompson *et al.* [15,16]. In the first one, the spatial lattice is dynamic, the transitions are discrete, and forces are used to calculate transitions probabilities. In the second one, pedestrians are described by three attached circles (an approximation to the human shape at the shoulders level) moving in a continuous space with velocities depending on the minimum interpersonal distance.

In the contractile particle model presented here, particles are allowed to move in the continuous space. The radii are dynamic variables that are recalculated depending on the distance to the neighbors. Also, the desired speed of each particle is calculated as a function of its radius. From the simulations, we compute the observables that will be compared to the experimental data reported in the literature.

The main macroscopic observables that characterize pedestrian dynamics are the fundamental diagram (which indicates the relationship between local density and average speed) and the specific flow rate (number of persons crossing an opening per unit of time and width). Regarding the fundamental diagram, a variety of experimental data have been reported in the literature [1,17–27] considering experiments and field observations in different situations and cultures. There are differences between these fundamental diagrams; nevertheless, all of them show a monotonically decreasing velocity as the density increases. Most legal regulations accept that the specific flow rate exhibited by a system of evacuating people in normal conditions remains constant, if the door width changes. Some regulations adopt a specific flow rate of 1.33 peds/(m s) (where “peds” stands for pedestrians) [28,29]. However, experimental results from the literature report different values for this magnitude ranging from 1.25 to 2 peds/(m s) [2,3,28–33] depending on the particular setup conditions, age, and culture of the population.

This work is organized as follows: In Sec. II the contractile particle model is presented. Section III shows simulation results of appropriate systems in order to compare them with the available empirical data in normal conditions, considering the fundamental diagram and the specific flow rate. It will be shown here that changes in the free parameters give enough

*dparisi@itba.edu.ar

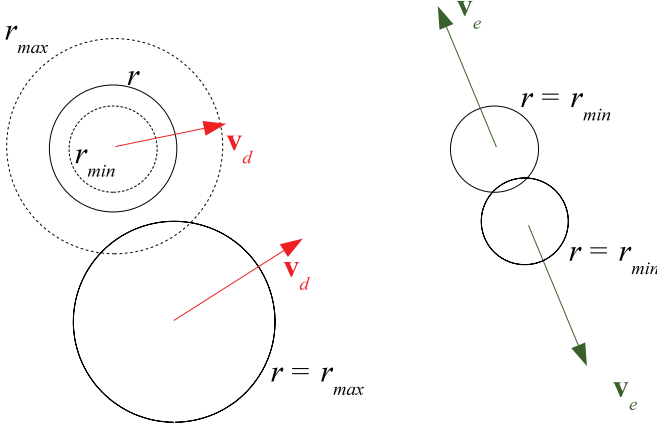


FIG. 1. (Color online) Illustration of the contractile particle model. Particles on the left are not in contact. They have no zero desired velocities (\mathbf{v}_d). Dashed circles represent the minimum and maximum radii. Particles on the right are in contact; therefore the escape velocities are present; also their radii are collapsed to the minimum.

flexibility to the model to allow adjusting the output to the different fundamental diagrams reported. In Sec. IV we present a parameter sensitivity analysis, which allows interpreting the fundamental diagram in terms of the microscopic parameters of the model. Finally, in Sec. V the conclusions are presented.

II. THE MODEL

The proposed contractile particle model has characteristics of both a continuous-space and a rule-based model. This allows describing trajectories and distance better than typical CA models [11] and besides, it allows improving the computing time compared with force-based models. This improvement is possible because forces are not calculated, there is no integration of the equations of motion, and consequently, the time step of the algorithm can be greater.

The basic components of the contractile particle model are the following: For each particle p^i ,

(1) The radius (r^i) is dynamically adjusted between r_{\min}^i and r_{\max}^i .

(2) It has a desired velocity (\mathbf{v}_d^i) pointing at the desired target location and its magnitude (v_d^i) represents the desired walking speed.

(3) The magnitude of the desired velocity is a function of the particle radius (r^i).

(4) If a particle (p^i) enters into contact with a boundary, an obstacle, or another particle, an escape velocity (\mathbf{v}_e^i) having a fixed magnitude (v_e) appears with direction and sense opposite to the interaction.

Figure 1 illustrates the geometry of these concepts.

The relation between the radius (r^i) and desired speed is such that $v_d(r_{\min}) = 0$, and $v_d(r_{\max}) = v_{d\max}$. We choose a functional form given by

$$v_d^i = v_{d\max} \left[\frac{(r^i - r_{\min})}{(r_{\max} - r_{\min})} \right]^\beta, \quad (1)$$

where $v_{d\max}$ is the desired speed at which a pedestrian would walk if she/he were unconstrained by any obstacle, i.e.,

walking free in an open space. If the exponent $\beta = 1$, then it is a linear relationship. For $\beta \neq 1$ the relationship has different curvature, either above the linear ($\beta < 1$) or below the linear ($\beta > 1$).

The time evolution is given in discrete time steps of

$$\Delta t = \frac{r_{\min}}{2 \max(v_{d\max}, v_e)}. \quad (2)$$

In each iteration the positions of particles are updated by the equation

$$\mathbf{x}^i(t) = \mathbf{x}^i(t - \Delta t) + \mathbf{v}^i(t)\Delta t \quad (3)$$

with

$$\mathbf{v}^i = \begin{cases} \mathbf{v}_d^i & \text{if } p^i \text{ is free of contact,} \\ \mathbf{v}_e^i & \text{otherwise,} \end{cases} \quad (4)$$

where the desired velocity is

$$\mathbf{v}_d^i = v_d^i \mathbf{e}_{\text{target}}^i, \quad (5)$$

and the versor $\mathbf{e}_{\text{target}}^i$ points toward some desired target location. The targets must be placed externally for each particular system to be simulated. As in other pedestrian models (such as in the social force model), the CPM does not provide a method for placing the targets automatically; this could be done by higher level algorithms that consider multiple factors such as way finding, decision making, efficient avoidance, etc.

The escape velocity can be written as

$$\mathbf{v}_e^i = v_e \frac{(\sum_j \mathbf{e}^{ij})}{|\sum_j \mathbf{e}^{ij}|}, \quad (6)$$

where \mathbf{e}^{ij} is the direction and sense of the escape velocity of particle p^i from every other particle or boundary in contact (j):

$$\mathbf{e}^{ij} = \frac{(\mathbf{x}^i - \mathbf{x}^j)}{|\mathbf{x}^i - \mathbf{x}^j|}. \quad (7)$$

In the case of interaction with a wall, \mathbf{x}^j indicates the nearest point on the wall to the center of particle p^i .

The rule for the variation of the radii is as follows: When a particle is not in contact with any other particle or boundary, its radius increases in each time step according to

$$\Delta r = \frac{r_{\max}}{\left(\frac{\tau}{\Delta t}\right)}, \quad (8)$$

where the constant τ characterizes the time taken for a particle to reach its maximum radius and thus its maximum velocity. We choose $\tau = 0.5$ s in accordance to the value used in the desired force in the social force model [8,34].

The radius increases until it reaches the maximum radius or the particle suffers a collision. In this last case, the particle tries to reduce the overlapping by diminishing its radius instantaneously to the minimum radius.

The following pseudocode describes the time evolution algorithm:

- Initialize boundaries and pedestrian positions and radii.
- iterate over time in steps of Δt

- iteration 1 over all particles
- Find contacts and calculate \mathbf{v}_e .
- end iteration 1
- iteration 2 over all particles
- Adjust radii following “the rule for the variation of the radii” [see text below Eq. (7)].
- end iteration 2
- iteration 3 over all particles
- Compute the direction and sense of the \mathbf{v}_d considering current positions and target locations.
- Compute the magnitude of \mathbf{v}_d depending on the radius following Eq. (1).
- end iteration 3
- iteration 4 over all particles

$$\mathbf{v}(t) = \mathbf{v}_d + \mathbf{v}_e = \begin{cases} \mathbf{v}_d^i & \text{if } r^i > r_{\min} \\ \mathbf{v}_e^i & \text{if } r^i = r_{\min} \end{cases}$$

$$\mathbf{x}(t) = \mathbf{x}(t - \Delta t) + \mathbf{v}(t)\Delta t$$

- end iteration 4
- end iteration over time

We must note that the variable radius is, in principle, a property of the model not directly related to any physical length. The variable radius is an effective radius considering several properties of the real system:

- (a) Pedestrians are not circles, they have a shoulder width greater than the anteroposterior length. Therefore, depending on the orientation and packing of the pedestrians within the crowd the effective radius can be different.
- (b) In this sense, r_{\min} is related to the equivalent radius so that a certain maximum density can be reached by a group of people.
- (c) On the other hand, a radius near r_{\max} is related to a sensor which regulates the minimum interpersonal distance at which the movement of a pedestrian begins to be affected by the presence of another pedestrian.

The escape velocity (\mathbf{v}_e) plays the role of an exclusion principle, preventing pedestrians from overlapping and bumping into obstacles and other pedestrians. If the magnitude $v_e < v_{d \max}$, an overlap of length ($v_{d \max} \Delta t$) cannot disappear in the next time step because the distance ($v_e \Delta t$) is smaller; then interacting particles would have $v_d = 0$ for at least two time steps. Smaller values of v_e will take more and more time steps (hence more time) to separate particles and, consequently, to start moving again with velocity $\mathbf{v} = \mathbf{v}_d$. In the limit when $v_e = 0$, pedestrians entering into contact would not move anymore.

Therefore, the parameter v_e can be interpreted as inversely related to a friction parameter which reduces the mobility of a system of particles by producing a sticking effect on them. For $v_e > v_{d \max}$, it will be shown in Sec. IV that the model behavior remains constant.

So, we choose for the model a fixed value of the escape speed

$$v_e = v_{d \max}. \quad (9)$$

The parameter $v_{d \max}$ is directly related to observed speeds of free pedestrians in different situations, and it can be easily adjusted in the model to reproduce the speed at nearly zero density in any particular system. Therefore, the free parameters

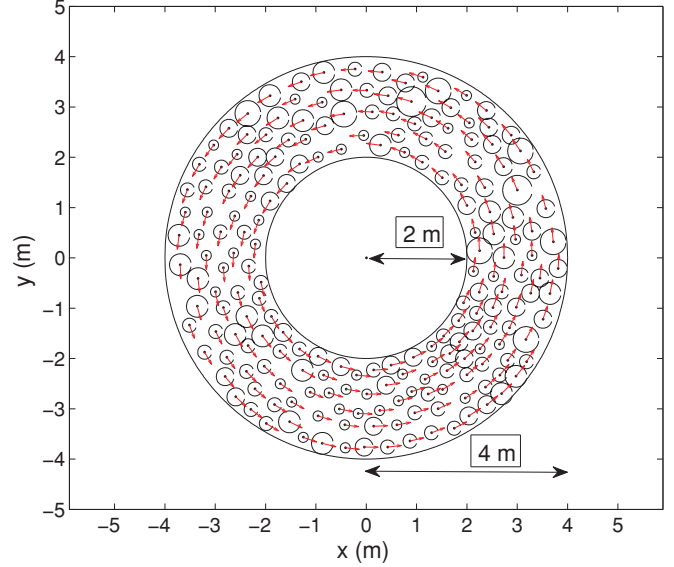


FIG. 2. (Color online) Simulated circular racetrack utilized to measure the fundamental diagram of pedestrian traffic. The arrows indicate the direction and sense of the desired velocities ($\mathbf{e}_{\text{target}}^i$).

of the model are r_{\min} , r_{\max} , and β , which can be tuned in order to reproduce empirical data.

An additional advantage of the proposed model is that it could also be adapted for simulating more general gravity-driven granular flows, given that the friction of particles can be adjusted by changing the parameter v_e .

III. SIMULATIONS AND RESULTS

We implement the proposed model to simulate two different scenarios: the movement of pedestrians in a circular racetrack and the egress from a room through a narrow door. The goal is to validate the model against experimental data reported in the bibliography. The first scenario allows calculating the fundamental diagram of simulated pedestrians and the second one enables the measurement of the specific flow rates.

A. Fundamental diagram

The geometry of the simulated system is a circular racetrack with an internal radius of 2 m and an outer radius of 4 m as shown in Fig. 2. Particles were initialized with uniform random position inside the circular geometry and with the variable radii set at $r^i = r_{\min}$ for all i . At all times the desired velocity of each particle is tangential to the racetrack (see Fig. 2). The number of pedestrians (N_p) in the circuit was varied to study the dynamics for different densities. Simulations with $N_p = 5, 10, \dots, 35, 45, 55, 65, \dots, 355$, and 365 particles were made.

For each density, one hundred realizations were performed; each one runs for 100 s. The positions and velocities of the particles in the system were recorded every 0.1 s, approximately ($\sim 2\Delta t$). The first 30 s of each simulation were discarded to ensure the system had reached its stationary state.

The density was calculated as the total number of particles (N_p) over the total area of the racetrack ($\rho = \frac{N_p}{12\pi}$). The velocity corresponding to that density was calculated by averaging over all particles and over time. The velocity of each particle was

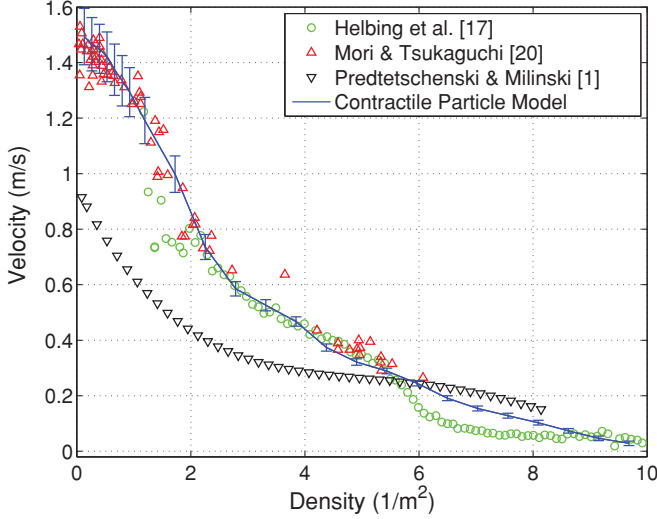


FIG. 3. (Color online) Experimental fundamental diagrams and the one obtained with the proposed model employing the “set of parameters 1”.

calculated as the projection of the instant velocity (4) onto the desired velocity (\mathbf{v}_d) (i.e., the vector tangential to the racetrack).

As stated in Sec. I, there exists a variety of reported empirical fundamental diagrams. Thus, we are going to use the flexibility of the model to reproduce some extreme curves. Published experimental data were taken from the public database at [25].

We call “set of parameters 1” the following model parameters:

$$\begin{aligned} r_{\min} &= 0.15 \text{ m}, \\ r_{\max} &= 0.32 \text{ m}, \\ \beta &= 0.9, \\ v_{d \max} &= 1.55 \text{ m/s}. \end{aligned}$$

Simulations using these parameters produce an output very similar to the fundamental diagrams reported in [17] and [20] as can be seen in Fig. 3.

Furthermore, changing to “set of parameters 2”

$$\begin{aligned} r_{\min} &= 0.10 \text{ m}, \\ r_{\max} &= 0.37 \text{ m}, \\ \beta &= 0.9, \\ v_{d \max} &= 0.95 \text{ m/s}, \end{aligned}$$

the model is able to approximate the data reported by Predtetschenskii and Milinskii [1] for densities up to 8 peds/m² as shown in Fig. 4.

The capacity of the proposed model for reproducing experimental data is remarkable. There are very few examples of this kind of comparison in the literature ([10], [34]) for any type of model; in particular, this has not been done before for rule-based (automata) models, as far as we know. The fact that different sets of parameters reproduce different fundamental diagrams allows interpreting the macroscopic differences in terms of the corresponding microscopic parameters.

Despite its simplicity, the CPM reproduce very well experimental data for low, medium, and high densities. However, it does not achieve a perfect fit near the stopping density. Experimental fundamental diagrams show in most cases a change of curvature before reaching the stopping density. This

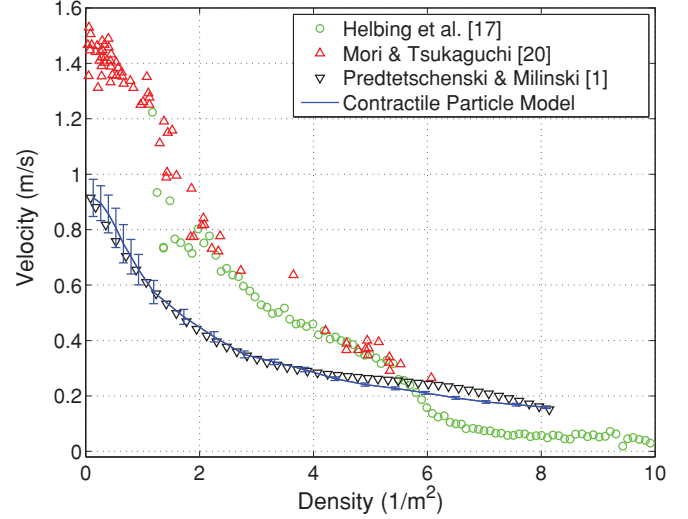


FIG. 4. (Color online) Experimental fundamental diagrams and the one obtained with the proposed model employing the “set of parameters 2”.

characteristic is not suitably reproduced by the model. In the case of the data reported in [17] a stopping density is not reached but there is a change of behavior near 6 peds/m² where a transition from laminar to turbulent flow is observed; also in this case the model does not account for this transition. Further investigations will be done in order to improve the CPM near the stopping density region.

B. Specific flow rate

Simulations of pedestrians leaving a 20 m × 20 m room with one exit were conducted to examine the specific flow rate exhibited by the contractile particle model. Particles inside the room have their targets located within the limits of the exit door in two possible ways. Let x be the horizontal coordinate where the exit door lies ($y = 0$); x_{e1} and x_{e2} are the left and right borders of the exit, respectively, and L is the exit width ($L = x_{e2} - x_{e1}$).

(a) If particle p^i has its x^i coordinate such that $x^i < (x_{e1} + 0.2L)$ OR $x^i > (x_{e1} + 0.8L)$, then the target is a random point in the interval $[x_{e1} + 0.2L, x_{e1} + 0.8L]$.

(b) Otherwise (if $x^i > x_{e1} + 0.2L$ AND $x^i < x_{e1} + 0.8L$) then the target is right below the particle ($x_{\text{target}}^i = x^i$).

In both cases the y component of the target is $y^i = 0$. Once a particle has reached the target at the exit, a new target is placed outside the room.

The initial positions of particles were uniformly distributed inside the room with their initial radii at r_{\min} in such a way the initial desired velocities were zero. Exit widths of $L = 1.2$ m, 2.7 m, and 3.2 m were considered for the room containing 200, 500, and 600 pedestrians, respectively. Increasing door width along with increasing number of pedestrians is used because in real systems, wider exits are required to evacuate more populated facilities. These values were chosen in accordance with the method of determining egress capacity stated in Chapter 7 of the *NFPA 101 Life Safety Code* (2000 edition), which indicates a minimum capacity factor of 0.5 cm per person.

In Fig. 5, some features of the egress simulation are shown: First, a snapshot of the egress process with $L = 1.2$ m and

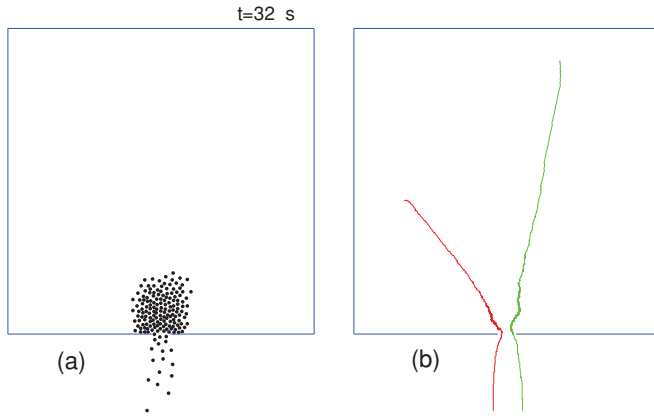


FIG. 5. (Color online) Details of one realization of the egress process with $L = 1.2$ m and “set of parameters 2”. (a) Snapshot of the process at $t = 32$ s. Each particle is represented by a dot; in the figure the size of the dot is fixed and similar to r_{\min} . (b) Two individual trajectories of two arbitrary particles.

set of parameters 2 is shown; second, individual trajectories of two arbitrary particles, of the same realization, are plotted. In the case of the snapshot it can be seen that the crowd before the door adopts a natural shape. Looking at the individual trajectories, it must be noted that they are realistic and that they show some slight fluctuation, which is less than 20 cm. This fluctuation originates with small corrections (at the microscopic level of the time step of the algorithm) produced by changes in the velocities due to the emergence of the escape velocity (\mathbf{v}_e) when particles enter into contact. It is worth remarking that in spite of the microscopic corrections given by \mathbf{v}_e , the observed macroscopic trajectories given by the CPM agree qualitatively with the observed pedestrian trajectories.

Now, in order to study the specific flow rate [measured as $N_p/(\text{Total Evacuation Time } L)$], the egress from the room was simulated by using the two sets of parameters found in the previous subsection and the three exit widths given above. For each configuration thirty realizations were performed. The mean values are plotted as a function of the exit widths (and the number of particles) in Fig. 6. In this figure, the following facts can be observed:

(a) The specific flow rate (Q_e) is nearly independent of the number of people, as is expected for normal conditions (this is also true for a fixed exit width and an increasing number of particles).

(b) For both sets of parameters, the values obtained of Q_e lie totally within the experimental range [1.25–2 peds/(m s)].

IV. PARAMETER SENSITIVITY ANALYSIS

In this section we are going to study the dependence of the proposed model on its parameters. First, let us analyze how variation of the microscopic parameters (r_{\min} , r_{\max} , and β) affect the fundamental diagram. Then we are going to study the specific flow rate as a function of the model parameter v_e .

As stated in previous sections, the magnitude $v_{d \max}$ can be easily determined by the speed of free pedestrians (the zero-density value of the fundamental diagram). Therefore, the other free parameters will be analyzed below. For each new parameter studied, simulations were performed following

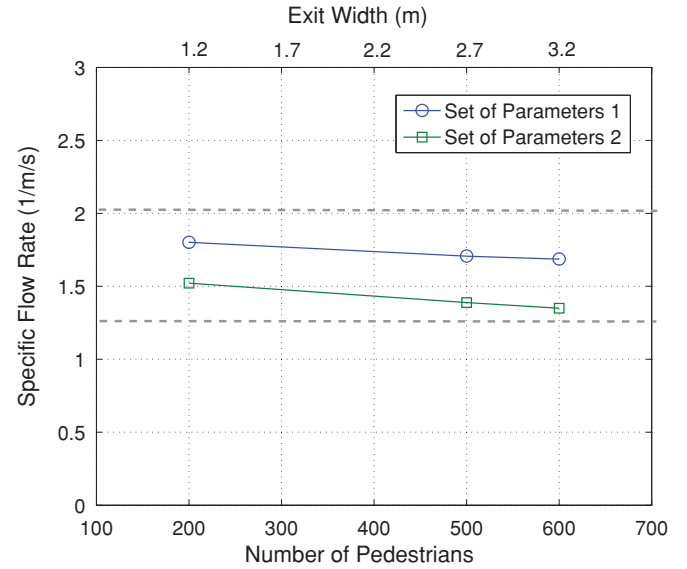


FIG. 6. (Color online) Specific flow rate obtained from the simulation of the egress of a $20 \text{ m} \times 20 \text{ m}$ room, with one exit. Number of people and exit width were varied accordingly (see text). Dashed lines indicate the experimental range. Errors lie between the symbol size.

the same specifications of the computational experiments (and of the racetrack system) described in Sec. III A.

In Fig. 7 it can be observed that changing only r_{\min} produces alterations in the high-density zone of the fundamental diagram. Decreasing r_{\min} gives as a result a greater stopping density and vice versa. This parameter can be associated with the minimal effective radius inside a packed crowd, which also allows tuning the maximum density reached by the simulated system. It is worth noting that for low and medium densities the curve does not change considerably; in particular, it remains invariant near $\rho = 2 \text{ peds/m}^2$ as this value is a crossing point for the three curves shown.

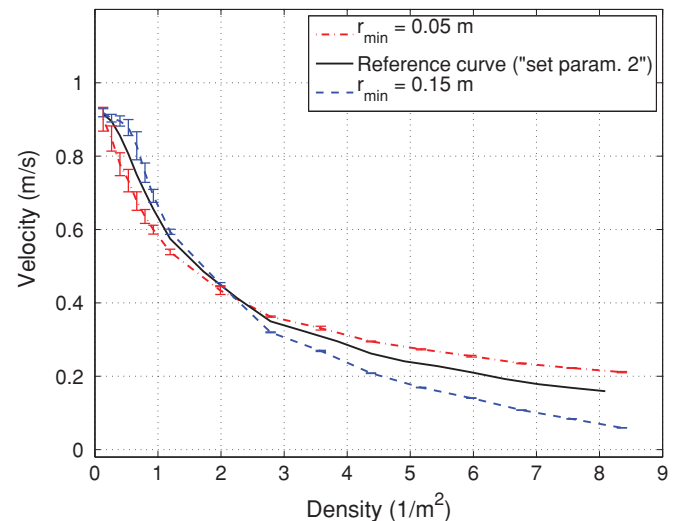


FIG. 7. (Color online) Influence of varying the free model parameter r_{\min} on the fundamental diagram.

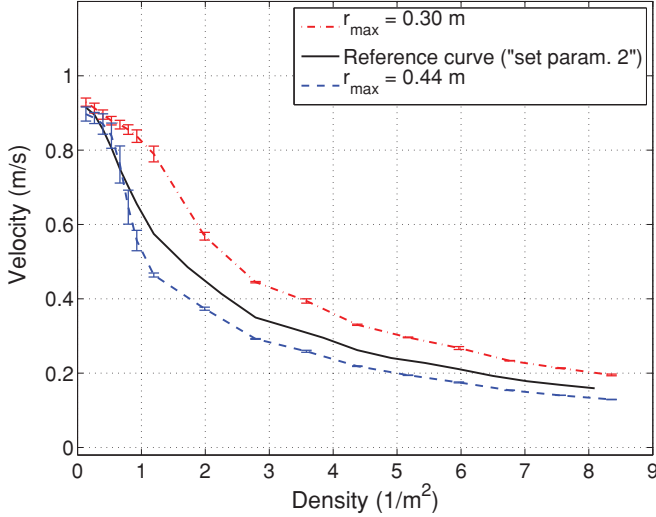


FIG. 8. (Color online) Effect of varying the free model parameter r_{\max} on the fundamental diagram.

When only the parameter r_{\max} is changed (Fig. 8) the impact on the high-density zone is very little; on the contrary, the curve at the low and medium density range (0.5–5 peds/m², in the present case) shows a major change. Hence, varying r_{\max} produces a complementary effect to that produced by changing r_{\min} . The parameter r_{\max} could be interpreted, at the microscopic level, as half of the minimum distance needed by a pedestrian to take a full-length walking step. Therefore we can state, in terms of the model, that this characteristic distance is responsible for the shape of the fundamental diagram at low and medium densities.

Figure 9 shows the influence of varying the form of the function relating the desired velocity and the radius of a given particle. This is achieved by changing the parameter β in Eq. (1). It can be observed a quasirigid rotation of the fundamental diagram around the fixed point at $\rho = 0$ and mean velocity equal to $v_{d \max}$. For the experimental data studied in Sec. III A it was found that the same $\beta = 0.9$ allows fitting very different empirical data suggesting that this parameter (and the pedestrian perception it represents) could be universal across a variety of fundamental diagrams.

Finally, we are going to study the dependence of simulation results on the model parameter v_e . As said in Sec. II, this parameter can increase or decrease the flow of particles by generating a sticking effect when v_e tends to zero. Figure 10 shows the specific flow rate of 200 pedestrians egressing from the room through an exit of 1.2 m and with the parameters given by set of parameters 1. As expected, it is observed that the specific flow rate approaches zero as v_e tends to zero. Also we can verify that Q_e does not change for $v_e > v_{d \max}$ ($=1.55$ m/s, in this case). This justifies the choice made in Eq. (9).

V. CONCLUSIONS

An automaton model for description of pedestrian dynamics was presented. The representation of the space and velocities is continuous, and transitions of state are governed by predefined rules (so it is not necessary to calculate forces), allowing the simulation of the evolution of the system in time steps of about

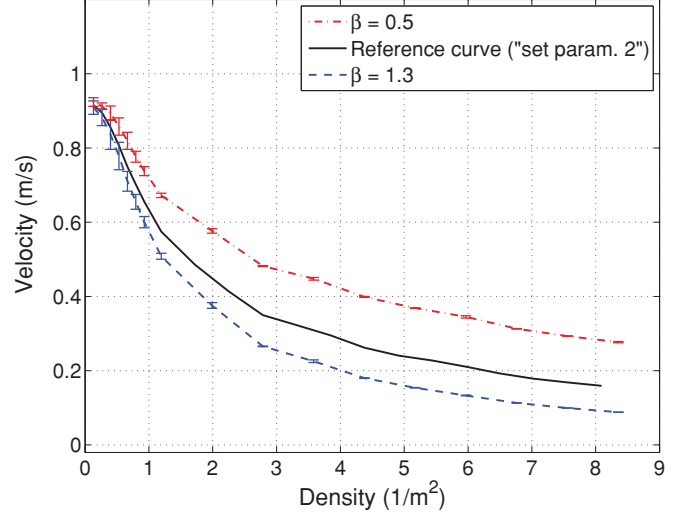


FIG. 9. (Color online) Impact of varying the model parameter β on the fundamental diagram.

0.05 s. This enhances considerably the speed of computation with respect to force-based models.

Pedestrians are described by bidimensional particles with variable radius between r_{\min} and r_{\max} . These are the relevant parameters of the model that can be adjusted in order to reproduce the available experimental data. In particular, the different fundamental diagrams of pedestrian traffic reported in the literature can be very well approximated by the proposed model, with the correct set of parameters. Furthermore, with the same parameters, the simulated specific flow rate of a group of people egressing through a narrow exit is in total agreement with the empirical data.

The flexibility of the model to adjust a wide range of fundamental diagrams by changing the two parameters r_{\min} and r_{\max} allows interpreting the difference between them in terms of these model parameters. Further investigation will be done in order to improve the fundamental diagram generated by the model in the stopping density zone.

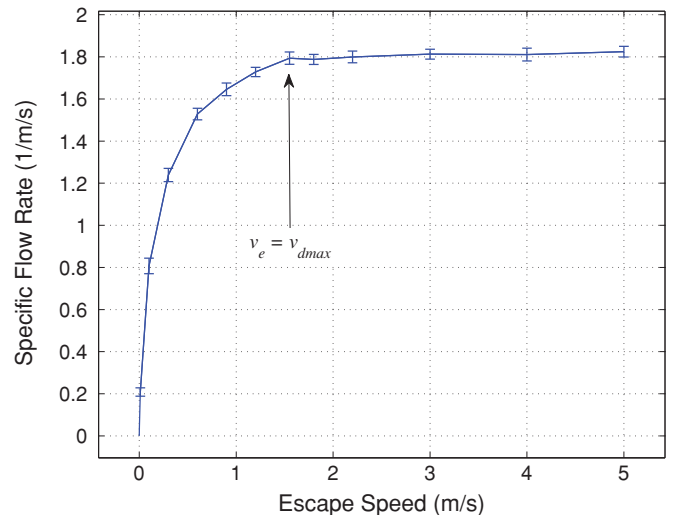


FIG. 10. (Color online) Variation of the specific flow rate as a function of the escape speed (v_e).

ACKNOWLEDGMENTS

This work was financially supported by CONICET (via Grant PIP 2010-2012, N 0304), ITBA, UNLP and ANPCyT

(Argentina). D. R. Parisi wants to thank Luciana Bruno and Victor Bettachini for useful discussion and suggestions.

-
- [1] V. M. Predtechenskii and A. I. Milinskii, *Planning for Foot Traffic Flow in Buildings*, published for the National Bureau of Standards, US Department of Commerce, and the National Science Foundation, Washington, DC (Amerind Publishing Company, New Dehli, 1978).
- [2] J. Fruin, *Pedestrian Planning and Design* (Metropolitan Association of Urban Designers and Environmental Planners, New York, NY, 1971).
- [3] B. D. Hankin and R. A. Wright, *Operational Res.* **9**, 81 (1958).
- [4] A. Schadschneider, W. Klingsch, H. Kluepfel, T. Kretz, C. Rogsch, and A. Seyfried, *Evacuation Dynamics: Empirical Results, Modeling, and Applications*, Encyclopedia of Complexity and System Science, edited by R. A. Meyers (Springer, Berlin, 2009), pp. 3142–3176.
- [5] A. Kirchner and A. Schadschneider, *Physica A* **312**, 260 (2002).
- [6] M. Muramatsu, *Physica A* **267**, 487 (1999).
- [7] D. Helbing and P. Molnar, *Phys. Rev. E* **51**, 4282 (1995).
- [8] D. Helbing, I. Farkas, and T. Vicsek, *Nature (London)* **407**, 487 (2000).
- [9] W. J. Yu, R. Chen, L. Y. Dong, and S. Q. Dai, *Phys. Rev. E* **72**, 026112 (2005).
- [10] M. Chraïbi, A. Seyfried, and A. Schadschneider, *Phys. Rev. E* **82**, 46111 (2010).
- [11] R. Guo and H. Huang, *Physica A* **387**, 580 (2008).
- [12] T. Vicsek, A. Czirók, E. Ben-Jacob, I. Cohen, and O. Shochet, *Phys. Rev. Lett.* **75**, 1226 (1995).
- [13] G. Baglietto and E. V. Albano, *Phys. Rev. E* **78**, 021125 (2008).
- [14] G. Baglietto and E. V. Albano, *Phys. Rev. E* **80**, 050103(R) (2009).
- [15] P. A. Thompson and E. W. Marchant, *Fire Safety Journal* **24**, 131 (1995).
- [16] P. Thompson, in NIST Workshop on Building Occupant Movement during Fire Emergencies, 2004, pp. 1–10.
- [17] D. Helbing, A. Johansson, and H. Al Abideen, *Phys. Rev. E* **75**, 046109 (2007).
- [18] A. Seyfried, B. Steffen, and T. Lippert, *Physica A* **368**, 232 (2006).
- [19] U. Weidmann, *Transporttechnik der Fussgänger, Transporttechnische Eigenschaften des Fussgängerverkehrs*, Schriftenreihe des IVT Nr. 90, 1993.
- [20] M. Mori and H. Tsukaguchi, *Transportation Research Part A, General* **21**, 223 (1987).
- [21] S. J. Older, *Traffic Engineering and Control* **10**, 160 (1968).
- [22] F. P. Navin and R. J. Wheeler, *Traffic Engineering (Inst. Traffic Eng.)* **39**, 30 (1969).
- [23] A. Seyfried, B. Steffen, W. Klingsch, and M. Boltesm, *J. Stat. Mech.: Theory Exp.* (2005) P10002.
- [24] P. J. DiNenno *et al.*, *SFPE Handbook of Fire Protection Engineering* (National Fire Protection Association, Quincy, MA, 2002).
- [25] H. Klüpfel, T. Kretz, C. Rogsch, A. Schadschneider, and A. Seyfried, [<http://www.ped-net.org>].
- [26] A. Seyfried, O. Passon, B. Steffen, M. Boltes, T. Rupperecht, and W. Klingsch, *Transportation Sci.* **43**, 395 (2009).
- [27] U. Chattaraj, A. Seyfried, and P. Chakroborty, *Advances in Complex Systems* **12**, 393 (2009).
- [28] Building Regulations, Approved Document B, Section B1, Department of the Environment and the Welsh Office, London, 1991.
- [29] Interim Guidelines for Evacuation Analyses for New and Existing Passenger Ships, Technical Report MSC/Circ. 1033, International Maritime Organization (IMO) Correspondence Group, 2002.
- [30] *The Green Guide, Guide to Safety at Sports Grounds*, 5th ed. (Department of Culture, Media, and Sport, United Kingdom, 2008).
- [31] D. Rasbash, G. Ramachandran, B. Kandola, J. Watts, and M. Law, *Evaluation of Fire Safety* (Wiley Online Library, 2004).
- [32] S. P. Hoogendoorn and W. Daamen, *Transportation Sci.* **39**, 147 (2005).
- [33] T. Kretz, A. Grünebohm, and M. Schreckenberg, *J. Stat. Mech.: Theory Exp.* (2006) P10014.
- [34] D. R. Parisi, M. Gilman, and H. Moldovan, *Physica A* **388**, 3600 (2009).